Investigation of the impact of wake modelling approaches on wind farm yield via yaw-based control optimization

Bartłomiej Paweł Rak

bartlomiejrak95@gmail.com

Instituto Superior Técnico, Universidade de Lisboa, Portugal

January 2021

Abstract: **The exploitation of offshore wind resources is considered to have tremendous potential in providing carbon-free energy. In order to increase the economic viability of wind farms, improvement in power generation is sought by mitigating the wake losses. While the industrial standards still favour turbine-level power maximization, a concept of collaborative yaw-based plant-level control has gained significant attention in recent years. This thesis investigates the potential of such a control strategy based on predictions of different wake modelling approaches under a range of atmospheric conditions and plant layouts. The utilized wake velocity deficit models are the top-hat Jensen model, the Gaussian-shaped Bastankhah model and its novel extension, termed Gauss–Curl Hybrid (GCH) model that accounts for secondary steering effects. The yaw control optimization is conducted on a row of eight NREL 5-MW turbines using the FLORIS modelling utility and SLSQP optimization algorithm. Generally speaking, the Jensen model shows lack of robustness and is not recommended for yaw control studies. In contrast, the two Gaussian-shaped models are well handled by the optimization algorithm and produce consistent results. More specifically, the Bastankhah model prefers yaw offsets of nearly equal magnitude throughout the whole wind farm except for the most downstream machine that remains aligned with the freestream. On the other hand, the GCH model suggests a large offset at the most upstream turbine, which is gradually reduced at consecutive machines. For a reference wind farm considered, the achieved power improvement yielded 3.59% and 14.66% for the Bastankhah and GCH models, respectively.**

Keywords: *Offshore Wind Energy, Wind Farm Optimization, Wind Farm Control, Wake Steering, Yaw Control, Wake Models*

I. INTRODUCTION

Wind energy production has experienced spectacular growth over the last decades marking this renewable resource as a recognised alternative to the conventional ways of electrical power generation [1]. While building large wind energy conversion systems helps to reduce the overall cost of energy due to many economies of scale, it introduces the problem of aerodynamic interaction between the machines via their wakes. The term "wake" refers to the volume of the flow affected by the kinetic energy extraction, that travels downstream of the turbine rotor. It is characterised by a reduced streamwise velocity, high vorticity and increased turbulence levels compared to the freestream conditions. The two major issues related to such aerodynamic coupling are reduced power output of downstream turbines and enhanced fatigue damage at the rotors. In the global scale, the wake effect contributes to considerable losses in power generation of wind farms as well as significantly increased operation and maintenance costs [2].

Many research efforts have been undertaken to decrease the adverse influence of wind turbine wakes through wind farm layout optimization. However, due to the unsteadiness of wind direction and externally imposed design restrictions, there is still a high occurrence of wake losses even for aerodynamically optimized wind plant layouts [2]. In the case of direct alignment between the wind direction and a row of turbines, the power loss at the second machine can amount to as much as 40%, showing a large potential for improvement [3]. Thus, alternative ways of reducing the wake losses are being sought by means of changing the wind farm control strategy.

The current industrial control standard still favours power maximization of each turbine alone, ignoring the negative effects that the machines have on one another through their wakes. As wind farms constantly grow in size and more knowledge on the wake effect has become available, the scientists' perception of the optimal wind farm control undergoes a paradigm shift, moving from so-called "greedy" into more collaborative inter turbine control methods [4].

In brief, this broad concept explores the possible ways of adjusting the available degrees of freedom of individual turbines to intentionally manipulate the wind field across the wind farm. This way a plant level objective of either power maximization or power set-point tracking with loads reduction can be achieved [5]. In recent years, yaw-based wake redirection technique has gained significant attention and is considered as a promising solution for the wake loss mitigation in existing and future wind farms, showing encouraging results obtained via simulations [6], wind tunnel experiments [7], and field tests [8].

The crucial aspect in assessing the viability of this control method is the ability to accurately predict the flow behaviour when the control actions are being implemented. For this purpose, various mathematical models capturing the wind turbine and wake aerodynamics are utilized. The main challenge within such an approach is associated with the credibility of the employed models, especially these accounting for the wake effects, which have stochastic nature and are still not fully understood. Thus, assessment of the reliability of the mathematical models in terms of capturing control-relevant wake behaviour and their impact on the suggested control actions remains an open research question [5].

This work aims to investigate the impact of three wake modelling approaches of various fidelity (Jensen, Bastankhah and Gauss-Curl Hybrid) on the solution of yaw-based plant-wise control optimization with the objective of farm yield maximization. It is of main interest to assess how characteristics of the employed models affect the resulting distribution of yaw settings and power gains at individual turbines under different wind conditions and fam layouts. The present investigation does not take into account the effect of the imposed yaw control settings and the resulting partial wake overlap situations on the loads experienced by the turbines. Steady-state wind farm simulations are carried out using a python-based control-oriented modelling framework FLORIS (FLOw Redirection and Induction in Steady-state) [6].

The remaining body of this paper is structured as follows. Section II introduces the concept of yaw-based wake redirection technique. Section III presents the applied methodology. Section IV is intended for the presentation and discussion of the results. Finally, in Section V the work is summarized and most important conclusions are drawn.

II. Yaw-based wake redirection

Wake steering approach consists of steering the wakes of upstream turbines away from the downstream ones, which can be achieved most effectively by operating the upstream machines with yaw angle offset [9], as shown in Figure 1. Due to the misalignment of the rotor axis with the incoming wind, the blades experience variable aerodynamic loads as they rotate. In the same time, the thrust force exerted on the wind, which acts perpendicularly to the rotor plane, creates an angle with the freestream wind direction. The resulting imbalance of loads and shifted direction of thrust impart an incident force that causes the wind to gain momentum in the crosswind direction and change its course of movement behind the turbine [10]. Further downstream the wake is influenced by a system of vortices released from the yawed rotor *i.e.* the wake rotation vortex and counter-rotating vortex pairs contributing to its deflection and deformation. As a result, the overlapping area between the deflected wake and a downstream turbine is reduced, leading to higher incident wind speed and consequently larger power output at the downstream machine. With the optimal yaw angle offset, the power output of a downstream turbine can exceed the yaw-induced losses of an upstream machine [11].
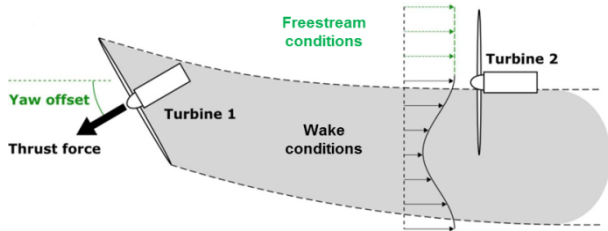

Figure 1 The concept of yaw-based wake steering [12]

An important aspect of yaw control studies is the definition of yaw angle direction. In this work, the positive yaw angle refers to the counter-clockwise rotation of the nacelle, when looking at the turbine from the top, with the wind coming from the left-hand side. Following this concept, the upstream turbine from Figure 1 is operating with a positive yaw angle offset.

III. Methodology

A. Wake modelling approaches

Three wake modelling approaches of different level of fidelity are employed in this study to account for the inter turbine aerodynamic effects. Due to the very limited space in this document, the mathematical formulations describing the flow field behind a turbine are not presented. However, all the necessary references are provided so that an interested reader can easily find the relevant equations. The wind farm aerodynamics is accounted for by the following set of models:

1) The Jensen wake velocity deficit model [13] that assumes uniform velocity deficit within the wake and constant wake growth rate, combined with the Jiménez wake deflection model [14, 6]

2) The Gaussian-shaped Bastankhah wake velocity deficit model [15] that accounts for atmospheric stability [16], operation in yaw [17] and rotor-added turbulence [18], further referred to as Gauss model, combined with the wake deflection model of the same author [17]

3) The Gauss-Curl Hybrid (GCH) wake velocity deficit model, which extends the Gauss model by accounting for yaw-added wake recovery and secondary steering effect [19], combined with the Bastankhah wake deflection model [17]

The wake superposition is captured by the widely known Park model [20] while the turbulence is handled with the Crespo-Hernández model [21] for each of the above combinations of velocity deficit and wake deflection models.

B. Simulation Setup

The study is conducted on a system of eight aligned NREL 5-MW reference turbines [22] and the scope of the examined yaw-control-relevant operating conditions was organized in the Simulation Matrix (Table 1). The abbreviations (w_s), (w_d), (T_I) and (spc) stand for wind speed, wind direction, turbulence intensity and spacing, respectively, where the spacing distance is expressed in terms of the rotor diameter (D = 126 [m]). According to the FLORIS convention, the freestream wind coming from 270° direction aligns with the row of turbines while a positive change in this value means a clockwise rotation of the freestream wind direction.

Table 1 Simulation Matrix

Case Name	Test variables			
	w_s [m/s]	w_d [°]	T_I [%]	spc [m]
Reference case (RC)	8	270	7.5	7D
High wind speed (HWS)	13	270	7.5	7D
Low wind speed (LWS)	5	270	7.5	7D
Wind direction 275° (WD_275)	8	275	7.5	7D
Wind direction 265° (WD_265)	8	265	7.5	7D
High turbulence intensity (HTI)	8	270	10	7D
Low turbulence intensity (LTI)	8	270	5	7D
Small spacing (SS)	8	270	7.5	5D
Large spacing (LS)	8	270	7.5	9D

C. Optimization Setup

In this study, the cumulative power of wind turbines is maximized with the yaw angle setting of each machine as a design variable. Since the present study does not take into account the yaw-induced loads, the bounds are set on the yaw angles so they would fall between $-50°$ and $+50°$. The SciPy optimization package [23] is employed for the optimization, using the Sequential Least SQuares Programming (SLSQP) minimization method developed by D. Kraft [24]. The optimization problem is defined as follows:

$$minimize\ P = -\sum_{i=1}^{N_t} P_i(\gamma_i) \qquad (1)$$

$$subject\ to -50° < \gamma_i < +50° \qquad (2)$$

where N_t is the number of turbines, P_i is the power and γ_i is the yaw angle setting of the *i-th* turbine. No equality or inequality constraints are prescribed in this formulation.

The initial vector of yaw angles $x0\_G$ was determined by manual manipulation of yaw setting at each turbine starting from the front one and checking the response of the whole system using the Jensen model. The yaw configuration with the largest power improvement found this way is:

$$x0\_G = [0, 27, 28, 28, 28, 28, 0, 0] \qquad (3)$$

Further, a sensitivity study on the relevant optimization parameters: function tolerance (f_tol), step size in gradient approximation (ε) and initial vector of design variables ($x0$) was conducted for each wake modelling method. The chosen values for these parameters were specified in Table 2.

Table 2 Summary of the optimization parameters

Wake model	f_tol [-]	ε [-]	$x0$ [°]
Jensen	10^{-13}	0.005	$x0\_G$
Gauss	10^{-13}	0.005	$x0\_G$
GCH	10^{-13}	0.02	$x0\_G$

Not being the main objective of this work, the sensitivity study showed a lack of robustness of the Jensen wake model over the whole range of tested parameters. This deficiency is believed to be due to the unrealistic assumption of uniform velocity deficit, which leads to misguiding gradient approximations and consequently randomness in the achieved optimization results. On the other hand, the Gauss and GCH wake models were consistent in their predictions independently of the applied optimization parameters, which suggests they are suitable for the studies of yaw control optimization.

IV. RESULTS ANALYSIS

A. Reference case

The reference case simulation parameters (w_s = 8 m/s, w_d = 270°, T_I = 0.075, spc = 7D) represent wind conditions of moderate speed and turbulence intensity, and direction aligned with the row of turbines. The wake losses amount to as much as 47.3% and 55.3% (-6 418 kW and -6 057 kW) versus the cumulative power of isolated turbines for the Jensen and Gauss / GCH wake models, respectively. It should be noted that the yaw-induced effects accounted for by the GCH wake model are effective only when a turbine operates in yaw misalignment. Therefore, simulation results with the baseline yaw settings are the same for the Gauss and GCH models. As a result of yaw control optimization, a new distribution of yaw settings is found for each wake modelling approach, as presented in Figure 2. Consequently, the power output at individual turbines has changed, as depicted in Figure. 3, leading to plant-wise power gains of 3.46 %, 3.59 % and 14.66 % for the Jensen, Gauss and GCH models, respectively, as summarized in Table 3 (P_{bsl} and P_{opt} denote farm power with baseline settings meaning zero yaw angle at each turbine, and optimized yaw settings, respectively, and ΔP the difference between them).
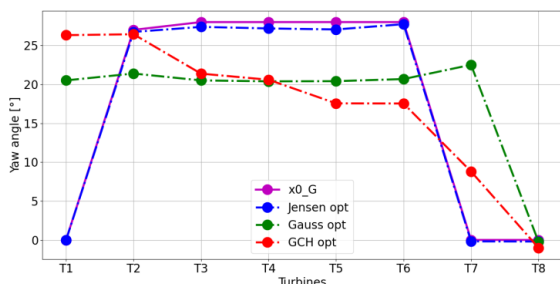

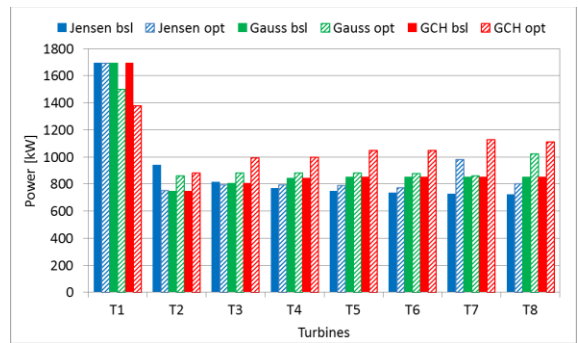Figure 2 Yaw distribution in x0_G and the optimization solutions – RC

Figure 3 Power distribution with baseline and optimized yaw settings – RC

Table 3 Summary of the results for the RC simulation

Wake model	P_{bsl} [kW]	P_{opt} [kW]	ΔP [%]
Jensen	7 145	7 393	3.46
Gauss	7 506	7 775	3.59
GCH	7 506	8 606	14.66

1) Optimal yaw control with the Jensen wake model

The new distribution of yaw settings is very similar to the optimization starting point ($x0\_G$). Although the largest power drop in relation to the nearest upstream turbine occurs at T2 (applied convention to refer to a specific turbine in the row), the optimizer does not suggest changing the yaw setting at T1. Presumably, the gains in power at T2 due to the partial wake overlap would not overcome the losses caused by yawing T1, which is slightly counter-intuitive. The reason for it is believed to be the uniform distribution of velocity deficit assumed in the Jensen model. The applied yaw misalignment at T2 – T6 yields approximately the value of +27° at each machine. However, the incident power output of these interior machines is either smaller (T3) or slightly larger (T4 – T6) compared to the baseline scenario. The power drop at T2 is solely caused by the operation in yaw while potential power gains due to partial wake overlap at T3 – T6 are compensated to continuously redirect the wake. It appears that the actual benefit from such yaw angles distribution is accumulated mainly at T7, which operates in partial wake overlap does not lose the power due to yawing (+160 kW vs baseline). Similarly, T8 remains aligned with the freestream and exposed to a combination of multiple redirected upstream wakes, which allows for increased power generation (+80 kW vs baseline).

2) Optimal yaw control with the Gauss wake model

As a result of the assumed Gaussian shape of the velocity deficit profile, yawing an upstream turbine even by a small angle immediately changes the inflow at the nearest downstream rotor. This, in contrast to the Jensen wake model, makes it beneficial to yaw T1, as less power has to be sacrificed to achieve higher incident wind speed at T2. The most favourable control strategy turns out to be keeping all the upstream turbines up to T7 yawed at around +20° and T8 aligned with the undisturbed wind. With such configuration, the major gains in power are at T2, T3 and T8 (+115 kW, +80 kW, +175 kW, respectively).

3) Optimal yaw control with the GCH wake model

The impact of the yaw-induced effects accounted for by the GCH model can be seen in the distribution of the optimal yaw settings. The largest yaw offset is applied at the first two machines and is being gradually reduced at the subsequent downstream turbines. Despite that, owing to the secondary

steering, the wake is being effectively redirected and the consecutive machines T2 – T8 report increasing power gains, that add up to +1410 kW and largely exceed the power loss due to yawing at T1 (-310 kW *vs* baseline). Interestingly, the optimal yaw angle at T8 is found to be -1° instead of the expected 0° angle.

B. High wind speed

The high wind speed simulation case parameters (w_s = 13 m/s, w_d = 270°, T_I = 0.075, spc = 7D) represent wind conditions for which the freestream wind velocity exceeds the rated speed of NREL 5-MW turbine (11.4 m/s). As a result, the wind farm power output is large while the wake losses amount to 14.9% and 21.5% (-5 927 kW and -8 558 kW) versus the cumulative power of isolated turbines for the Jensen and Gauss / GCH wake models, respectively. The solution of yaw control setpoints optimization for each wake modelling approach and the resulting power changes at the individual turbines were presented in Figure 4 and Figure 5, respectively, with the cumulative impact summarized in Table 4.

1) Optimal yaw control with the Jensen wake model

The plant-wise power gain of 2.55 % (+865 kW *vs* baseline) is reported with the optimal yaw control strategy applied. A large yaw offset of +34° is proposed for T1, and a smaller amounting to +24° for T2, both ensuring maximum deflection while still operating at rated power. For some reason, the optimal yaw angle at T3 is found to be -13° and the remaining turbines are aligned with the wind direction, which is a bit unintuitive. Thanks to such yaw setpoints distribution, T2 and T3 switch to operation at rated power, T4 reports significant power gain (+467 kW *vs* baseline) while T5 increases its power by +156 kW *vs* baseline.

2) Optimal yaw control with the Gauss wake model

Employing the Gauss wake model for yaw control optimization results in the total wind farm power increase of 7.27% (+2 277 kW *vs* baseline). Again, the largest yaw angle is applied at T1 with the same magnitude which is suggested with the Jensen model. In fact, as T1 is exposed to the undistrubed wind it is expected that this machine will apply the same yaw offset regardless of the utilized wake modelling approach. Despite applying a +20° yaw angle, T2 still operates at rated power (+500 kW *vs* baseline) while T3 is significantly yawed in the opposite direction (-24°) and reports power increase of +445 kW *vs* baseline. It is not understandable why particularly T3 exhibits such behaviour. It appears that it was the best setting in terms of plant-wise benefits that the optimization algorithm could find. As opposed to the predictions using the Jensen wake model, the further downstream turbines apply a yaw angle misalignment of around +20°, while the last one is aligned with the freestream. The resulting power gains are distributed among T4, T5, T7 and T8, with the latter one contributing the most due to lack of yaw-induced power losses.

3) Optimal yaw control with the GCH wake model

The total power gain reported when GCH model is employed amounts to as much as 16.42% (+5 139 kW *vs* baseline), considerably exceeding the results obtained with the other models. Consistently with previous observations, T1 is yawed at +34° and produces rated power. The yaw misalignment at T2 yields +22° and increases to 24° at T3. Then, a gradual drop in yaw offset is seen at the subsequent turbines. The incident power gains at the individual turbines range between +400 kW to nearly 1.1 MW throughout the wind farm. The impact of the secondary steering effect is very noticeable, especially at the rear turbines that effectively redirect the wake with

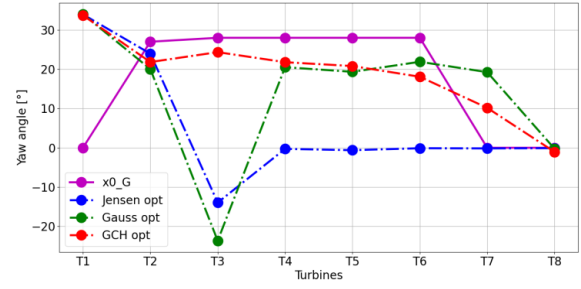successively smaller applied yaw errors while showing increasing power gains.

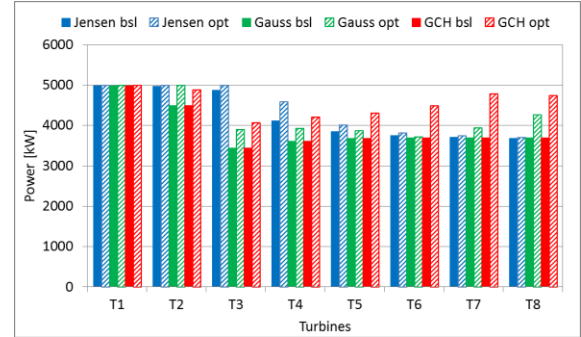*Figure 4 Yaw distribution in x0_G and the optimization solutions – HWS*

Figure 5 Power distribution with baseline and optimized yaw settings – HWS

Table 4 Summary of the results for the HWS simulation

Wake model	P_{bsl} [kW]	P_{opt} [kW]	ΔP [%]
Jensen	33 934	34 799	2.55
Gauss	31 303	33 580	7.27
GCH	31 303	36 442	16.42

C. Low wind speed

The low wind speed simulation case (w_s = 5 m/s, w_d = 270°, T_I = 0.075, spc = 7D) intends to assess the applicability of yaw control in a wind farm exposed to wind resource of poor energy content and unfavourable direction. The wake losses under present wind conditions are 74.5% and 48.3% (-2 292 kW and -1 487 kW) versus the cumulative power of isolated turbines for the Jensen and Gauss / GCH wake models, respectively. The optimal yaw configurations are shown in Figure 6 while the power outputs of individual turbines and the whole wind farm are presented in Figure 7 and Table 5, respectively.

1) Optimal yaw control with the Jensen wake model

The magnitude of power improvement achieved with the Jensen wake model is relatively large (+547 kW *vs* baseline). The resulting yaw settings indeed effectively redirect the wake creating partial wake overlap at the downstream machines, which in turn bring about large power gains at the successive machines. However, in the light of such small baseline farm yield and the limitations of the Jensen model, the credibility of such an outcome in a real wind farm is doubtful.

2) Optimal yaw control with the Gauss wake model

Based on the results obtained for the Gauss wake model in terms of both the total power gain (+15 kW vs baseline) and the yaw angles distribution, it appears that the application of yaw control is not beneficial at low wind speeds.
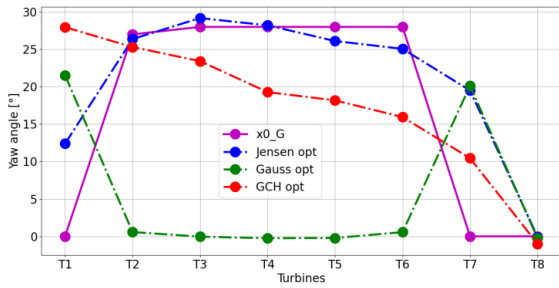
4

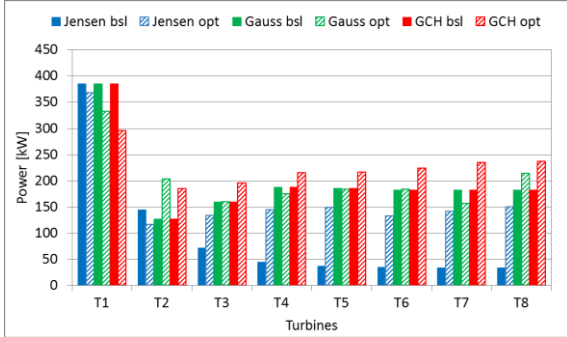Figure 6 Yaw distribution in x0_G and the optimization solutions – LWS

Figure 7 Power distribution with baseline and optimized yaw settings – LWS

Table 5 Summary of the results for the LWS simulation

Wake model	P_{bsl} [kW]	P_{opt} [kW]	ΔP [%]
Jensen	785	1 332	69.61
Gauss	1 591	1 606	0.95
GCH	1 591	1 799	13.11

3) Optimal yaw control with the GCH wake model

The resulting distribution of optimal yaw settings is consistent with the previous predictions using the GCH model. A gradually decreasing yaw offset applied at subsequent turbines brought about a total power gain of 13.11% (+108 kW *vs* baseline).

D. Wind direction 275°

The wind direction 275° simulation case parameters (w_s = 8 m/s, w_d = 275°, T_I = 0.075, spc = 7D) represent a situation when partial wake overlap is naturally achieved. As a consequence, the turbines operating with baseline yaw control generate more power (+1 792 kW for Jensen and +2 722 kW for Gauss / GCH) compared to the RC baseline results. However, the farm power loss due to the wake effect is still present and amounts to 34.1% and 24.6% (-4 626 kW and -3 335 kW) versus the cumulative power of isolated turbines for the Jensen and Gauss / GCH wake models, respectively. The suggested yaw control settings are presented in Figure 8, the power outputs of individual turbines in Figure 9 while total farm power is summarized in Table 6.
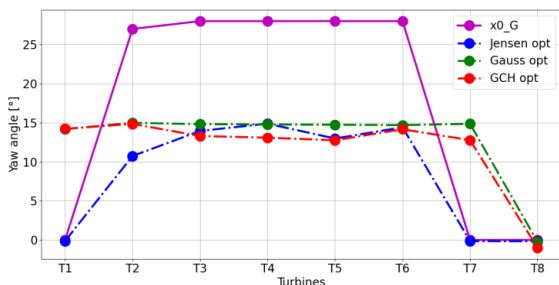

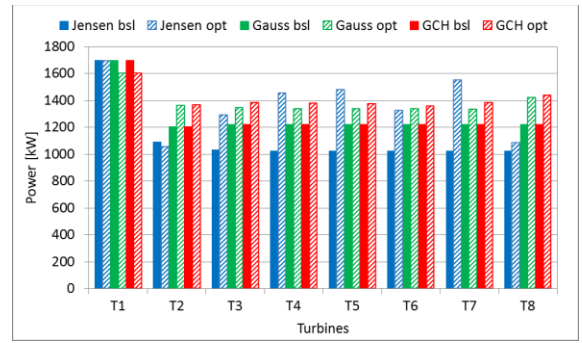Figure 8 Yaw distribution in x0_G and the optimization solutions – WD_275

Figure 9 Power distribution with baseline and optimized yaw settings – WD_275

Table 6 Summary of the results for the WD_275 simulation

Wake model	P_{bsl} [kW]	P_{opt} [kW]	ΔP [%]
Jensen	8 937	10 941	22.42
Gauss	10 228	11 084	8.37
GCH	10 228	11 291	10.40

1) Optimal yaw control with the Jensen wake model

The reported total power gain with the optimal yaw control settings yields 22.42 % (+2 004 kW *vs* baseline) and is the largest improvement among the considered wake models under present wind conditions. Similarly to the RC simulation results, T1, T7 and T8 are selected to remain aligned with the freestream wind while the interior machines T2 – T6 are yawed by the angle between 10° and 15°. Such yaw settings distribution results in an even larger partial wake overlap operating conditions at T3 – T7, which in turn brings about significant power gains at these turbines. In this scenario, only a small fraction of power at T2 is sacrificed (-35 kW *vs* baseline). Understandably, the present wind direction is favourable for yaw control using Jensen's wake characteristics as the region of inconsequent yawing that is required before a partial wake overlap situation at a downstream rotor is achieved is completely omitted.

2) Optimal yaw control with the Gauss wake model

The predicted plant-wise power improvement due to the optimized yaw control using the Gauss wake modelling method yields 8.37 % (+856 kW *vs* baseline). The overall pattern of the yaw angles distribution very well resembles the one obtained in the RC simulation with a difference that the optimized yaw settings applied at T1 – T7 are approximately 15° at each machine. Consequently, the downstream machines T2 – T8 are exposed to higher effective wind velocity and generate more power. The achieved power improvement is significantly larger compared to the RC simulation. The reason behind it lies in the accumulation of velocity deficit is in the centre of the Gaussian wake, which is effectively redirected outside of the downstream turbines' rotor swept area.

3) Optimal yaw control with the GCH wake model

Employing the GCH wake model for the optimization of yaw setpoints results in the total power improvement of 10.4 % (+1 063 kW *vs* baseline). For the simulations with both Gauss and GCH wake models, the power drop at T2 (-90 kW *vs* baseline) is reported. Also, the obtained distributions of the optimized yaw angles are similar, however, with a modest decrease in the magnitude at T3 – T5 and T7 due to the impact of secondary steering effect. This in turn makes the power gains at individual machines larger than those achieved with the Gauss model.

However, it is important to notice that the impact of the secondary steering is not as considerable as it was in the RC simulation with full wake overlap at each downstream rotor.

E. Wind direction 265°

The wind direction 265° simulation (w_s = 8 m/s, w_d = 265°, T_I = 0.075, spc = 7D) intends to examine the applicability of yaw control when the partial wake overlap is naturally achieved but the wake is shifted to the opposite direction than in WD_275°. Both the predicted baseline power and the associated wake losses are exactly the same as in WD_275° simulation. However, it is of interest to observe if such a change in wind direction impacts the results of yaw control optimization. The new yaw settings configurations are presented in Figure 10, the power predictions of individual machines in Figure 11 and total wind farm power summarized in Table 7.

1) Optimal yaw control with the Jensen wake model

Interestingly, a larger achieved farm power gain of 25.37% (+2 267 kW *vs* baseline) is reported using the Jensen wake model than in WD_275° simulation. This finding is very interesting given that both the Jensen and Jiménez models do not account for any effects that could lead to a different velocity field predictions depending on the direction of yaw misalignment. The suggested optimal yaw settings are noticeably different compared to WD_275° simulation. Here, the first turbine is yawed by -5°, the latter T2 – T5 yaw approximately by -15°, T6 is yawed by -21°, T7 by +7° and lastly T8 by +1.5°. The power gains are accumulated in the interior turbines, with the largest at T7. However, it is not clear why T7 and T8 apply positive yaw angles as it is certain to bring only power losses.

2) Optimal yaw control with the Gauss wake model

The magnitude of wind farm power improvement obtained with the Gauss wake modelling approach corresponds to that achieved in WD_275° simulation. The yaw angles distribution in the park is the same but with the opposite sign while the resulting power gains at individual turbines are identical as for WD_275° conditions. Based on the knowledge of the model, this is expected behaviour since this wake modelling method does not account for any effects related to the direction of yawing.

3) Optimal yaw control with the GCH wake model

Although the achieved level of farm power improvement is nearly the same as in WD_275° simulation, the incident distribution of the yaw settings is a bit different for the GCH wake model. As expected, the yaw angles at T1 – T7 become negative, however, the magnitude of yaw errors applied at T2, T3, T5-T7 increases by 1.5° to 3°. This suggests that larger yaw misalignment has to be set to achieve nearly the same power as for WD_275° conditions. In other words, it appears that yawing in the negative direction is less effective, which is attributed to the impact of wake rotation vortex.
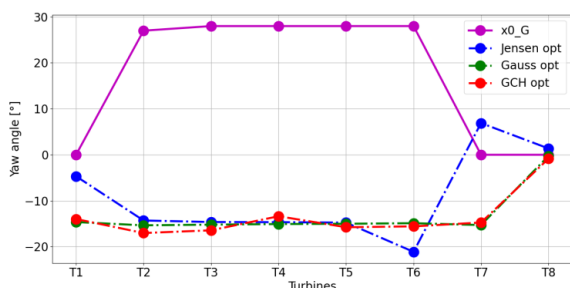

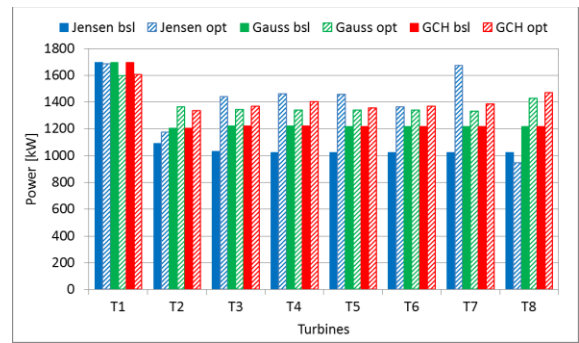*Figure 10 Yaw distribution in x0_G and the optimization solutions – WD_265*

Figure 11 Power distribution with baseline and optimized yaw settings – WD_265

Table 7 Summary of the results for the WD_265 simulation

Wake model	P_{bsl} [kW]	P_{opt} [kW]	ΔP [%]
Jensen	8 937	11 204	25.37
Gauss	10 228	11 084	8.37
GCH	10 228	11 300	10.48

F. High turbulence intensity

The high turbulence intensity simulation case parameters (w_s = 8 m/s, w_d = 270°, T_I = 0.1, spc = 7D) represent wind conditions characterized by moderate speed, unfavourable wind direction and increased freestream turbulence. It is known that higher turbulence levels positively affect the wake recovery rate due to better turbulent mixing of the flow within the wake with the undisturbed wind. However, many old and strongly simplified wake models, like the one proposed by Jensen, do not directly account for the effect of the turbulence intensity. A common practice is to adjust the wake recovery constant so that the predicted wake resembles better the behaviour of the factual wake under given turbulence intensity level. On the other hand, the Gauss and GCH wake models account for both the turbulence intensity in the freestream and the added turbulence coming from the nearest upstream rotor. The incident turbulence level is then used to determine the local wake growth rate, which eventually affects the width of the Gaussian shape in spanwise and vertical directions as well as the magnitude of the velocity deficit inside the wake at a given downstream distance. The wind farm power prediction for baseline and optimized yaw control setpoints is summarized in Table 8. The present wake losses amount to 47.3% and 38% (-6 418 kW and -5 156 kW) versus the cumulative power of isolated turbines for the Jensen and Gauss / GCH wake models, respectively. An apparent farm power gain (+901 kW) due to increased turbulence level can be observed for the greedy yaw control using Gauss / GCH wake models compared to the respective scenarios from RC simulation. The proposed yaw control setpoints are shown in Figure 12 while the power generation at individual turbines is presented in Figure 13.
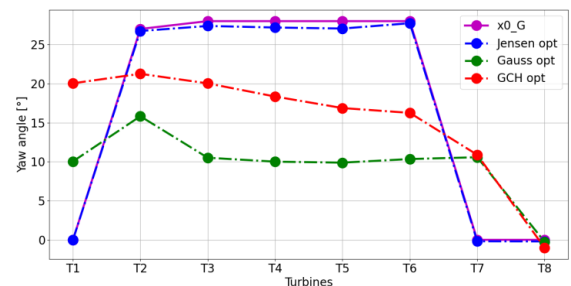

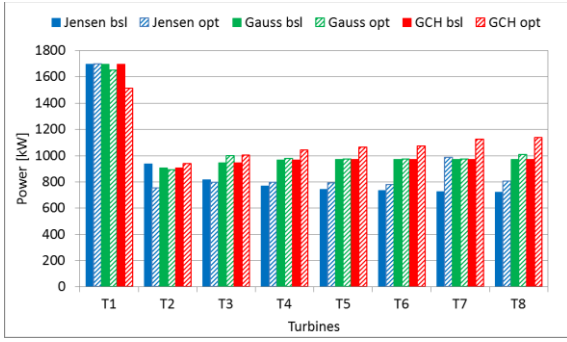*Figure 12 Yaw distribution in x0_G and the optimization solutions – HTI*

Figure 13 Power distribution with baseline and optimized yaw settings – HTI

Table 8 Summary of the results for the HTI simulation

Wake model	P_{bsl} [kW]	P_{opt} [kW]	ΔP [%]
Jensen	7 145	7 393	3.46
Gauss	8 407	8 430	0.27
GCH	8 407	8 884	5.67

1) Optimal yaw control with the Jensen wake model

Since the Jensen wake model does not directly account for the impact of turbulence within the flow, the optimization results are identical as those reported in the RC simulation. The assumption of the constant wake growth rate is likely unrealistic in the light of the present knowledge on the wake aerodynamics. This example shows the evident limitation of the Jensen wake model in terms of its application in studying yaw-based wake redirection wind farm control.

2) Optimal yaw control with the Gauss wake model

A very poor power improvement of 0.27 % (+23 kW *vs* baseline) is achieved for the Gauss wake modelling method. Due to the increased wake recovery rate, the effective wind speeds at the downstream turbines are substantially larger with the baseline yaw control when compared to the RC simulation. The distribution of the optimal yaw angles indicates that smaller yaw offsets are preferred, resulting in a small wake deflection. Taking into account the resulting distribution of power output achieved at individual turbines and the magnitude of the total power improvement, it is questionable whether the use of yaw wake redirection method is beneficial under highly turbulent winds. It appears that the gains in power caused by redirecting the wake are compensated by the yaw-induced power losses.

3) Optimal yaw control with the GCH wake model

The combined impact of the applied yaw errors and the secondary steering effect results in a substantial power gain of 5.67 % (+477 kW *vs* baseline). The overall pattern of the optimized yaw settings distribution resembles the one obtained in the RC simulation. Larger yaw offsets are preferred at T1 – T3, which are reduced at the subsequent turbines to reach -1° at T8. The distribution of power output along the turbines follows the opposite trend to one of the yaw angles. Power at T1 is sacrificed (-183 kW *vs* baseline) but is easily compensated by the gains at the remaining machines (+660 kW in total *vs* baseline).

G. Low turbulence intensity

The low turbulence intensity simulation case parameters (w_s = 8 m/s, w_d = 270°, T_I = 0.05, spc = 7D) characterize wind of moderate speed, unfavourable direction and low freestream turbulence intensity. Such operating conditions are especially

adverse in a real wind farm since in addition to the full wake overlap situations at the downstream rotors the wake recovery rate is reduced. In the present simulation, the wake losses amount to 47.3% and 52.4% (-6 418 kW and -7 104 kW) versus the cumulative power of isolated turbines for the Jensen and Gauss / GCH wake models, respectively. In contrast to HTI simulation case, here an apparent farm power loss (-1 047 kW) due to reduced turbulence level can be observed for the greedy yaw control using Gauss / GCH wake models compared to the respective scenarios from RC simulation. The optimized yaw setpoints and power output at individual turbines are presented in Figure 14 and Figure 15, respectively while total farm power is summarized in Table 9.
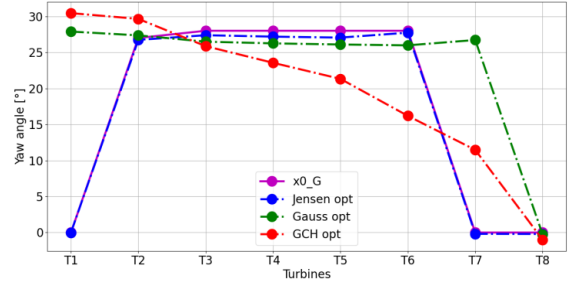

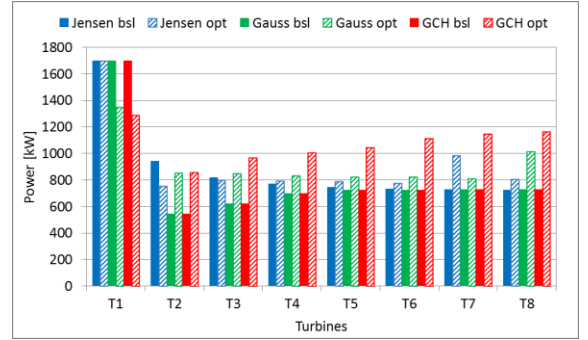*Figure 14 Yaw distribution in x0_G and the optimization solutions – LTI*

Figure 15 Power distribution with baseline and optimized yaw settings – LTI

Table 9 Summary of the results for the LTI simulation

Wake model	P_{bsl} [kW]	P_{opt} [kW]	ΔP [%]
Jensen	7 145	7 393	3.46
Gauss	6 459	7 343	13.69
GCH	6 459	8 584	32.89

1) Optimal yaw control with the Jensen wake model

The findings regarding the yaw control optimization using the Jensen wake modelling method, under different turbulence levels, elaborated in the HTI simulation case, equally apply to the present LTI test. No further comments on this matter will be made.

2) Optimal yaw control with the Gauss wake model

In contrast to what was observed in the HTI simulation case, a satisfying power improvement of 13.69% (+884 kW *vs* baseline) is achieved with the Gauss wake model employed. Relatively large yaw angle offsets, exceeding +25°, are proposed for T1 – T7 while T8 remains aligned with the freestream. Such increased magnitude stems from the fact that the velocity deficit at downstream turbines' rotors is enlarged. More specifically, the incident wind speeds are lower and the wake region where these velocity deficits are accumulated is wider. Therefore, yawing the machines by larger yaw angles is

still advantageous in terms of overall power gains. A significant yaw-induced power drop at T1 was reported (-350 kW *vs* baseline), which is almost completely compensated already at T2 (+305 kW *vs* baseline).

3) Optimal yaw control with the GCH wake model

An outstanding power improvement was reported when yaw optimization was conducted using the GCH wake model. The total power gain reaches as much as 32.89% (+2 125 kW *vs* baseline) with large yaw angle offset applied at T1, which is gradually reduced at the consecutive machines. The resulting overall pattern of the yaw angles distribution very well resembles one obtained in LWS simulation case, where the magnitude of the wake loss within the park is also significant. The impact of the yaw-induced features captured by this model is substantial in the present scenario.

H. Small spacing

The small spacing simulation case parameters (w_s = 8 m/s, w_d = 270°, T_I = 0.075, spc = 5D) represent the same wind conditions as in the RC simulation, however, the aerodynamics of the wind farm is affected by a smaller spacing distance between the machines. Due to such configuration, the wake travels a shorter distance before it hits the consecutive turbine, which limits its level of recovery. Based on the results summarized in Table 10 it is evident that the total power output is reduced compared to respective RC simulation results with the greedy settings and the magnitude of power drop yields 25% (-1 843 kW) for the Jensen and 21.5% (-1 613 kW) for the Gauss / GCH wake models. In the present scenario, the wake losses with baseline yaw settings are significant, amounting to 61% and 56.6% (-8 261 kW and -7 670 kW) versus the cumulative power of isolated turbines for the Jensen and Gauss / GCH wake models, respectively. The proposed yaw angles configurations and the power generated by individual turbines are presented in Figure 16 and Figure 17, respectively.

1) Optimal yaw control with the Jensen wake model

Employment of the wake model proposed by Jensen results in an increase of total power generation by 17.86% (+947 kW *vs* baseline) when the yaw control set points are optimized. The incident distribution of yaw angles very closely follows the pattern of the initial guess of the vector *x0_G*. Similarly to the RC simulation, the power drop due to operation in yaw is reported at T2 (-168 kW *vs* baseline) whereas growing gains are obtained at further downstream machines. It appears that either the x0_G was a good guess of the optimization starting point or the optimization algorithm was trapped around the initially imposed solution.

2) Optimal yaw control with the Gauss wake model

Wind farm power improvement of 11.48% (+676 kW *vs* baseline) is achieved when the yaw optimization was run with the Gauss wake model. Unlike for the Jensen wake model, the resultant yaw angle distribution is noticeably different than the one obtained in the RC simulation. The yaw angle settings fall between 25° and 31° for T1 – T7, creating a saw shape, and remain 0° at T8. A clear correlation can be observed between the distribution of yaw settings and distribution of power output at individual machines. The largest power gains are reported T3, T6, and T8, being the nearest downstream machines behind T2, T5 and T7, which operate with yaw error of over 30°. As a result of the smaller spacing distance and the associated larger velocity deficits experienced by the downstream machines, in general, greater yaw angle offsets are proposed, which is consistent with the engineering intuition.
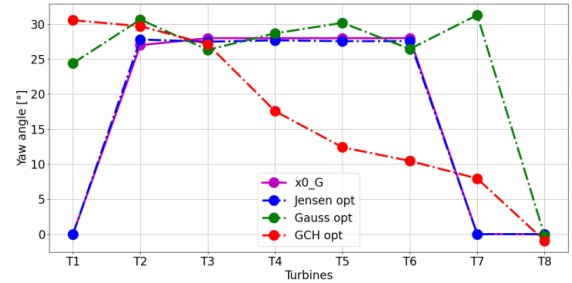

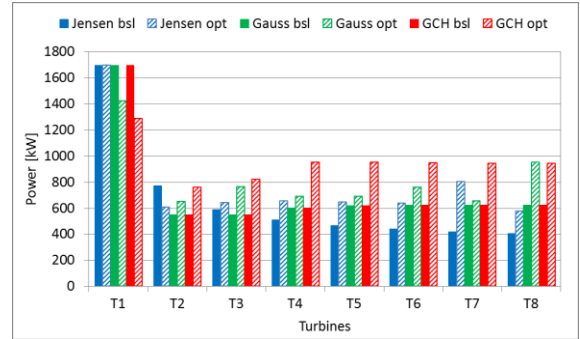*Figure 16 Yaw distribution in x0_G and the optimization solutions – SS*

Figure 17 Power distribution with baseline and optimized yaw settings – SS

Table 10 Summary of the results for the SS simulation

Wake model	P_{bsl} [kW]	P_{opt} [kW]	ΔP [%]
Jensen	5 302	6 249	17.86
Gauss	5 893	6 569	11.48
GCH	5 893	7 590	28.80

3) Optimal yaw control with the GCH wake model

The plant-wise power gain of 28.8% (+2 697 kW *vs* baseline) is obtained with the GCH wake modelling method employed. It is also the only scenario in which the optimized wind farm power reaches the magnitude of the baseline total power in the RC simulation. The yaw distribution starts with large, slowly decreasing yaw errors applied at the front turbines, T1 – T3. Then, a more pronounced reduction in yaw is observed at T4, which shrinks at the subsequent machines, T5 – T7, to again become significant at T8. Consequently, considerable power gains at individual turbines, especially T4 – T8 are achieved. According to the predictions with GCH wake model, the reduced spacing distance created a great potential for improving the power of the system via collaborative yaw control strategy.

I. Large spacing

The large spacing simulation (w_s = 8 m/s, w_d = 270°, T_I = 0.075, spc = 9D) intends to evaluate the applicability of yaw-based wake redirection when the turbines are spaced further apart. In contrast to SS simulation, now the wake travels a longer distance before it hits the consecutive turbine, which enhances its level of recovery. The results summarized in Table 11 show that the total power output of the wind farm with 9D spacing and greedy settings is improved compared to the respective RC simulations. The magnitude of improvement amounts to 18% (+1 282 kW) for the Jensen and 17% (-1 258 kW) for the Gauss / GCH wake models. Consequently, the wake losses experienced with baseline yaw control are reduced and yield 37.9% and 35.4% (-5 136 kW and -4 799 kW *vs* the power of isolated turbines) for the Jensen and Gauss / GCH wake models, respectively. The optimized yaw control

setpoints are shown in Figure 18 while the achieved power output at the individual machines is presented in Figure 19.
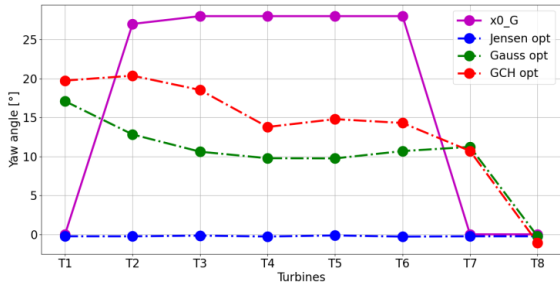

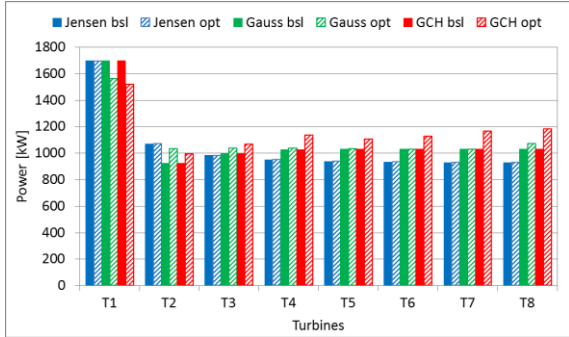*Figure 18 Yaw distribution in x0_G and the optimization solutions – LS*

Figure 19 Power distribution with baseline and optimized yaw settings – LS

Table 11 Summary of the results for the SS simulation

Wake model	P_{bsl} [kW]	P_{opt} [kW]	ΔP [%]
Jensen	8 427	8 427	0.00
Gauss	8 764	8 818	0.61
GCH	8 764	9 277	5.85

1) Optimal yaw control with the Jensen wake model

No change in the yaw settings, and consequently no power improvement is suggested when the Jensen model is used. It appears that the wake recovers enough so that it is not advantageous to sacrifice the power by yawing the machines to create partial wake overlap situations at the downstream rotors. Based on the previous observations of the impact of Jensen's wake characteristics on yaw control optimization, it is an understandable behaviour.

2) Optimal yaw control with the Gauss wake model

For the simulation with the Gauss wake modelling approach, a small total power improvement is achieved, amounting to 0.61% (+54 kW *vs* baseline). The suggested yaw settings start with 17° misalignment at T1 that is gradually reduced at further turbines until T4 and T5, which both yaw by 10°. Then, the magnitude of yaw offset rises insignificantly at T6 and T7 and remains 0° at T8. The yaw-induced power loss of -133 kW at T1 is reported, which is barely compensated with the power gains at the remaining downstream turbines. Given the level of achieved improvement in this test, the benefit of plant-wise yaw control application for further spaced turbines is questionable.

3) Optimal yaw control with the GCH wake model

A satisfying level of total power gain, amounting to 5.85% (+513 kW vs baseline) is obtained for the simulation with the GCH wake model. Although the wake is more recovered, due

to the impact of the secondary steering it is still advantageous to implement yaw-based wake redirection.

V. CONCLUSIONS

In this work, a collaborative yaw-based wake steering approach to control a wind farm under various wind conditions and layouts was investigated. Three wake modelling approaches of different level of fidelity (Jensen, Gauss, Gauss-Curl Hybrid) were employed to account for the aerodynamic interference between the machines. The objective of the study was to investigate the impact of the applied wake modelling method on the solution of yaw control optimization with the purpose of maximizing power generation of a wind park. The most important conclusions drawn from this study are stated below.

Regarding the application of the Jensen wake model in the present work, several deficiencies of this simple model were found. First, it was observed that in situations when the wind direction is aligned with the turbines, there is always a certain scope of "idle" yawing an upstream turbine that is needed to reach the transition point between full and partial wake overlap condition at a nearest downstream rotor. As a consequence, the upstream machine loses power according to the $\cos^2 \gamma$ rule of thumb while the downstream one experiences meaninglessly low gains only because the upstream machine extracted less energy. This range of unproductive yawing was checked for RC simulation conditions and amounted to 14° with the associated power loss of 5.3% at the upstream turbine. Due to such behaviour, the Jensen model gives a very unrealistic flow field prediction, which is especially unacceptable when the objective is to achieve power improvement by manipulating yaw angles. In contrast, in WD_275° and WD_265° simulations, the impact of "idle" yawing was naturally mitigated resulting in very large power gains predicted with the Jensen model, which supports the above statements. Secondly, this simple model doesn't directly account for the turbulence intensity level, which was proven to have a significant impact on the applicability of yaw control. Overall, plant-wise power gains were reported for 8 out of 9 simulations, however, in four (RC, HTI, LTI, SS) the resulting yaw distribution is nearly the same as in x0_G vector. Moreover, in the LS case, the greedy control is suggested while in another three cases (HWS, LWS, WD_265°) the credibility of the optimization results is doubtful. Taking into account the limitations of Jensen's model, the yaw control proposed in WD_275° simulation is to some extent satisfying. Besides, the only consistency in the prediction of optimal yaw settings distribution was that the last turbine should remain aligned with the freestream. In light of the above findings, it is concluded that the Jensen wake model is not suitable for wind farm optimization studies that rely on yaw control.

The Bastankhah model assuming the Gaussian profile of the wake velocity deficit was found to be much more suitable for yaw control optimization than the Jensen model. Due to its higher fidelity level, the improvement was seen in terms of both the performance of the optimization algorithm and robustness in wind farm aerodynamics predictions under varied atmospheric conditions and park layouts. The yaw angles adjustments proposed by the optimizer were consistent and sensible throughout the whole study. According to the predictions made with this model, encouraging power improvement was observed for six tests (RC, HWS, WD_275°, WD_265°, LTI, SS) while for the remaining three (LWS, HTI, LS) the benefits of yaw-based wake steering implementation were doubtful. These results are aligned with the common conjecture that yaw control is applicable only when the wake

losses are significant. With few exceptions, it was noticed that a nearly constant yaw distribution was proposed for T1 – T7, with the magnitude dependent on the simulation parameters, while the last machine was always aligned with the freestream. In the reference wind farm considered, a power gain of 3.59% (+270 kW) was achieved with the following yaw angle misalignments distribution [20.5 21.5 20.5 20.5 20.5 20.5 22.5 0] compared to operation with the greedy turbine-level control strategy.

Regarding the application of the Gauss-Curl Hybrid model, good performance of the optimization algorithm was observed together with robust wind farm aerodynamics predictions. The incorporation of the yaw-induced features of this model resulted in very promising farm power gains for all of the conducted yaw optimization cases. In general, due to the enhanced wake deflection and recovery, this wake modelling approach promotes larger yaw offset at the front turbine, which is being gradually reduced at the consecutive machines. Such behaviour is aligned with the engineering intuition, with an exception that it is not clear why the last turbine is always yawed by -1° angle instead of being aligned with the undisturbed wind. In the reference wind farm considered, a power gain of 14.66% (+1 100 kW) was achieved with the following yaw setpoints distribution [26.5 26.5 21.5 20.5 17.5 17.5 9 -1] compared to operation with the greedy turbine-level control strategy. Based on the results obtained with this model, it appears that the inclusion of the secondary steering effect has a game-changing impact in terms of the potential for yield increase and yaw misalignment distribution of collaborative WF control.

VI. Acknowledgements

VII. References

[1] IRENA, "Future of wind: Deployment, investment, technology, grid integration and socio-economic aspects (a global energy transformation paper)," International Renewable Energy Agency, Abu Dhabi, Tech. Rep., 2019.

[2] J. F. Herbert-Acero, O. Probst, P.-E. Réthoré, G. C. Larsen, and K. K. Castillo-Villar, "A review of methodological approaches for the design and optimization of wind farms," *Energies*, vol. 7, no. 11, pp. 6930–7016, 2014.

[3] R. J. Barthelmie, O. Rathmann, S. T. Frandsen, K. Hansen, E. Politis, J. Prospathopoulos, K. Rados, D. Cabezón, W. Schlez, J. Phillips *et al.*, "Modelling and measurements of wakes in large wind farms," in *Journal of Physics: Conference Series*, vol. 75, no. 1. IOP Publishing, 2007, p. 012049.

[4] K. E. Johnson and N. Thomas, "Wind farm control: Addressing the aerodynamic interaction among wind turbines," in *2009 American Control Conference*. IEEE, 2009, pp. 2104–2109.

[5] S. Boersma, B. Doekemeijer, P. M. Gebraad, P. A. Fleming, J. Annoni, A. K. Scholbrock, J. Frederik, and J.-W. van Wingerden, "A tutorial on control-oriented modeling and control of wind farms," in *2017 American Control Conference (ACC)*. IEEE, 2017, pp. 1–18.

[6] P. M. Gebraad, F. Teeuwisse, J. Van Wingerden, P. A. Fleming, S. Ruben, J. Marden, and L. Pao, "Wind plant power optimization through yaw control using a parametric model for wake effects - a cfd simulation study," *Wind Energy*, vol. 19, no. 1, pp. 95–114, 2016.

[7] J. Schottler, A. Hölling, J. Peinke, and M. Hölling, "Wind tunnel tests on controllable model wind turbines in yaw," in *34th wind energy symposium*, 2016, p. 1523.

[8] P. Fleming, J. King, K. Dykes, E. Simley, J. Roadman, A. Scholbrock, P. Murphy, J. K. Lundquist, P. Moriarty, K. Fleming *et al.*, "Initial results from a field campaign of wake steering applied at a commercial wind farm–part 1," *Wind Energy Science (Online)*, vol. 4, no. NREL/JA-5000-73991, 2019.

[9] S. Kanev, F. Savenije, and W. Engels, "Active wake control: An approach to optimize the lifetime operation of wind farms," *Wind Energy*, vol. 21, no. 7, pp. 488–501, 2018.

[10] T. Burton, N. Jenkins, D. Sharpe, and E. Bossanyi, *Wind energy handbook*. John Wiley & Sons, 2011.

[11] P. Fleming, P. M. Gebraad, S. Lee, J.-W. van Wingerden, K. Johnson, M. Churchfield, J. Michalakes, P. Spalart, and P. Moriarty, "Simulation comparison of wake mitigation control strategies for a two-turbine case," *Wind Energy*, vol. 18, no. 12, pp. 2135–2143, 2015.

[12] A. C. Kheirabadi and R. Nagamune, "A quantitative review of wind farm control with the objective of wind farm power maximization," *Journal of Wind Engineering and Industrial Aerodynamics*, vol. 192, pp. 45–73, 2019.

[13] N. O. Jensen, *A note on wind generator interaction*. Risø National Laboratory, 1983.

[14] Á. Jiménez, A. Crespo, and E. Migoya, "Application of a les technique to characterize the wake deflection of a wind turbine in yaw," *Wind energy*, vol. 13, no. 6, pp. 559–572, 2010.

[15] M. Bastankhah and F. Porté-Agel, "A new analytical model for wind-turbine wakes," *Renewable Energy*, vol. 70, pp. 116–123, 2014.

[16] M. Abkar and F. Porté-Agel, "Influence of atmospheric stability on wind-turbine wakes: A large-eddy simulation study," *Physics of fluids*, vol. 27, no. 3, p. 035104, 2015.

[17] M. Bastankhah and F. Porté-Agel, "Experimental and theoretical study of wind turbine wakes in yawed conditions," *Journal of Fluid Mechanics*, vol. 806, pp. 506–541, 2016.

[18] A. Niayifar and F. Porté-Agel, "Analytical modeling of wind farms: A new approach for power prediction," *Energies*, vol. 9, no. 9, p. 741, 2016.

[19] J. King, P. Fleming, R. King, L. A. Martnez-Tossas, C. J. Bay, R. Mudafort, and E. Simley, "Controls-oriented model for secondary effects of wake steering," *Wind Energy Science Discussions*, vol. 2020, pp. 1–22, 2020. [Online]. Available: https://www.wind-energ-sci-discuss.net/wes-2020-3/

[20] I. Katic, J. Højstrup, and N. O. Jensen, "A simple model for cluster efficiency," in *European wind energy association conference and exhibition*. A. Raguzzi, 1987, pp. 407–410.

[21] A. Crespo, J. Hernandez *et al.*, "Turbulence characteristics in wind-turbine wakes," *Journal of wind engineering and industrial aerodynamics*, vol. 61, no. 1, pp. 71–85, 1996.

[22] J. Jonkman, S. Butterfield, W. Musial, and G. Scott, "Definition of a 5-mw reference wind turbine for offshore system development," National Renewable Energy Lab.(NREL), Golden, CO (United States), Tech. Rep., 2009.

[23] E. Jones, T. Oliphant, P. Peterson *et al.*, "Scipy: Open source scientific tools for python," 2001.

[24] D. Kraft, "A software package for sequential quadratic programming." DLR German Aerospace Center – Institute for Flight Mechanics, Koln, Germany, techreport DFVLR-FB 88-28, 1988.